# Phase-coded microwave signal generation based on a single electro-optical modulator and its application in accurate distance measurement

**Fangzheng Zhang, Xiaozhong Ge, Bindong Gao and Shilong Pan***

*Key Laboratory of Radar Imaging and Microwave Photonics, Ministry of Education, Nanjing University of Aeronautics and Astronautics, Nanjing 210016, China*

**pans@ieee.org*

**Abstract:** A novel scheme for photonic generation of a phase-coded microwave signal is proposed and its application in one-dimension distance measurement is demonstrated. The proposed signal generator has a simple and compact structure based on a single dual-polarization modulator. Besides, the generated phase-coded signal is stable and free from the DC and low-frequency backgrounds. An experiment is carried out. A 2 Gb/s phase-coded signal at 20 GHz is successfully generated, and the recovered phase information agrees well with the input 13-bit Barker code. To further investigate the performance of the proposed signal generator, its application in one-dimension distance measurement is demonstrated. The measurement accuracy is less than 1.7 centimeters within a measurement range of ~2 meters. The experimental results can verify the feasibility of the proposed phase-coded microwave signal generator and also provide strong evidence to support its practical applications.



**OCIS codes:** (060.5625) Radio frequency photonics; (060.5060) Phase modulation; (280.5600) Radar.

## References and links

1. D. K. Barton, *Radar System Analysis and Modeling* (Artech House, 2005).
2. G. Ungerboeck, "Channel coding with multilevel/phase signals," IEEE Trans. Inf. Theory **28**(1), 55–67 (1982).
3. R. F. Holloway, W. H. Weedon, B. Houshmand, and R. Roll, "Next generation W-band radar testbed," Radar Conference, 65–71 (2007).
4. S. M. Gu, C. Li, X. Gao, Z. Y. Sun, and G. Y. Fang, "Terahertz aperture synthesized imaging with fan-beam scanning for personnel screening," IEEE Trans. Microw. Theory Tech. **60**(12), 3877–3885 (2012).
5. R. C. Daniels and R. W. Heath, Jr., "60 GHz wireless communications: emerging requirements and design recommendations," IEEE Vehicular Technology Magazine **2**(3), 41–50 (2007).
6. X. Li, J. Yu, J. Zhang, F. Li, Y. Xu, Z. Zhang, and J. Xiao, "Fiber-wireless fiber link for 100 Gb/s PDM-QPSK signal transmission at W-band," IEEE Photonics Technol. Lett. **26**(18), 1825–1828 (2014).
7. H. J. Song and T. Nagatsuma, ""Present and future of terahertz communications" IEEE Trans. THz Sci," Technol. **1**(1), 256–263 (2011).
8. J. Chou, Y. Han, and B. Jalali, "Adaptive RF-photonic arbitrary waveform generator," IEEE Photonics Technol. Lett. **15**(4), 581–583 (2003).
9. A. M. Weiner, "Ultrafast optical pulse shaping: A tutorial review," Opt. Commun. **284**(15), 3669–3692 (2011).
10. F. Zhang, X. Ge, S. Pan, and J. Yao, "Photonic generation of pulsed microwave signals with tunable frequency and phase based on spectral-shaping and frequency-to-time mapping," Opt. Lett. **38**(20), 4256–4259 (2013).
11. Z. Li, W. Li, H. Chi, X. Zhang, and J. Yao, "Photonic generation of phase-coded microwave signal with large frequency tenability," IEEE Photonics Technol. Lett. **23**(11), 712–714 (2011).
12. H. Y. Jiang, L. S. Yan, J. Ye, W. Pan, B. Luo, and X. Zou, "Photonic generation of phase-coded microwave signals with tunable carrier frequency," Opt. Lett. **38**(8), 1361–1363 (2013).
13. H. Chi and J. Yao, "Photonic generation of phase-coded millimeter-wave signal using a polarization modulator," IEEE Microw. Wirel. Compon. Lett. **18**(5), 371–373 (2008).
14. Z. Li, M. Li, H. Chi, X. Zhang, and J. P. Yao, "Photonic generation of phase-coded millimeter-wave signal with large frequency tenability using a polarization-maintaining fiber Bragg grating," IEEE Microw. Wirel. Compon. Lett. **21**(12), 694–696 (2011).
15. S. Liu, D. Zhu, Z. Wei, and S. Pan, "Photonic generation of widely tunable phase-coded microwave signals based on a dual-parallel polarization modulator," Opt. Lett. **39**(13), 3958–3961 (2014).

#242351 Received 4 Jun 2015; revised 29 Jul 2015; accepted 7 Aug 2015; published 12 Aug 2015

16. Y. Chen, A. Wen, Y. Chen, and X. Wu, "Photonic generation of binary and quaternary phase-coded microwave waveforms with an ultra-wide frequency tunable range," Opt. Express **22**(13), 15618–15625 (2014).
17. P. Lu, D. Liu, D. Huang, and J. Sun, "Study of temperature stability for fiber-optic Mach-Zehnder interferometer filter," in Proceedings of the 3rd International Conference on Microwave and Millimeter Wave Technology (ICMMT 2002), 1087–1089 (2002).
18. A. H. Gnauck, R. W. Tkach, A. R. Chraplyvy, and T. Li, "High-capacity optical transmission systems," J. Lightwave Technol. **26**(9), 1032–1045 (2008).
19. H. B. Voelcker, "Toward a unified theory of modulation part I: phase-envelope relationships," Proc. IEEE **54**(3), 340–353 (1966).

## 1. Introduction

Phase-coded signals have wide applications in radar and communication technologies [1, 2]. In modern radar and communication systems, the operation frequency is developing towards the high frequency bands. For example, W-band (75-110 GHz) and terahertz band (300GHz-3THz) radars with unique advantages have been intensively developed in recent years [3, 4]. Meanwhile, wireless communications in high frequency bands such as the 60 GHz band [5], W-band [6] and terahertz band [7] are also developing rapidly. In these systems, broadband phase-coded signal is always preferred. Phase-coded pulse compression has been widely used in radar systems, where a large signal bandwidth can help to achieve a high range resolution [1]. Therefore, broadband phase-coded signal is of great significance to improve the ability of discrimination for radar. In communication systems, the signal bandwidth is also increasing to meet the demand for high speed data transmissions, e. g., communication by a 4-level phase-coded W-band signal with a bandwidth of more than 10 GHz is demonstrated in a fiber-wireless system [6]. However, the phase-coded signal generated in electrical domain using a direct digital synthesizer (DDS) has a low carrier frequency and its bandwidth is usually limited to several gigahertz. Although the generated signal can be moved to a higher frequency band through electrical frequency up-conversion, this would not only increase the complexity but also introduce excess amplitude and phase distortions to the signal.

To deal with the above problems, photonic technologies are proposed to generate phase-coded microwave signals with the advantages such as extremely high frequency, large bandwidth (tens of gigahertz), low loss and small size, etc [8]. Among all the schemes for photonic generation of phase-coded microwave signals, one method is realized by optical spectral shaping and frequency-to-time mapping [8–10]. This method can achieve adaptive waveform generation if the spectral shaping is implemented by a programmable spatial light modulator, but the system is complicated with a large size and high coupling loss due to the use of free-space optic devices. Besides, the temporal aperture of the generated phase-coded microwave signal is usually limited (< 1us), which may hinder its usage in some applications. Furthermore, due to the square-law detection in the photodetector (PD), the DC and many low frequency components exist in the generated signals [10], which would decrease the power efficiency and also cause interference to other frequency bands. The second method for photonic phase-coded microwave signal generation is achieved by controlling the phase difference between two coherent optical carriers followed by frequency heterodyning at a PD [11–16]. In this method, the two coherent optical carriers with different wavelengths are usually generated by driving an electro-optical modulator (EOM) with a radio frequency (RF) signal. Then, the two carriers are separated either in the frequency domain using wavelength selective devices [11, 12] or in the polarization domain using polarization dependent devices [13–15]. After that, one of the optical carriers is phase modulated by the coding signal before the two carriers are combined again and sent to a PD. The system based on this principle is usually complicated. For example, in [12], a Mach-Zehnder modulator (MZM) is first applied to generate two optical carriers. The two carriers are separated through a circulator together with a fiber Bragg grating (FBG) and then, one of the carriers is phase modulated at a phase modulator (PM) before they are combined and sent to a PD. In [15], two polarization modulators and five polarization controllers are used to generate two optical carriers in orthogonal polarizations, and a third polarization modulator is followed to introduce a phase difference between the two optical carriers. It can be found that, at least two EOMs and a few other optical devices are required in these schemes to implement optical carrier generation,

#242351 Received 4 Jun 2015; revised 29 Jul 2015; accepted 7 Aug 2015; published 12 Aug 2015

separation and modulation, which results in a sophisticated structure and a high cost. Another problem with this method is that, independent operation of the separated optical carriers using non-integrated devices would degrade the stability of the generated phase-coded signal. As demonstrated in [16], the optical source is split into two branches by an optical coupler. One branch is phase modulated by the coding signal, and the other branch is frequency-shifted by a dual-parallel Mach Zehnder modulator (DPMZM). A phase-coded microwave signal can be generated when the two branches are combined and sent to a PD. In this scheme, independent operation of the two separated optical carriers through different fiber branches will degrade the phase coherence and thus deteriorate the stability of the generated signal [17].

In this paper, we propose a novel scheme for photonic generation of a phase-coded microwave signal based on a dual-polarization modulator and balanced photodetection. Compared with the previous photonic schemes, the proposed scheme has a very simple structure using only a single compact and integrated modulator. All the optical carrier manipulations are implemented inside the integrated modulator, thus a stable phase-coded signal can be obtained. In addition, the generated phase-coded signal is free from the DC and low-frequency backgrounds thanks to the balanced photodetection. An experiment is carried out, and the feasibility of the proposed signal generator is experimentally verified. To further investigate the performance of the proposed phase-coded signal generator, its application in one-dimension distance measurement is demonstrated, which is rarely reported in the previous reports on photonic generation of phase coded microwave signals.

## 2. Phase-coded microwave signal generation

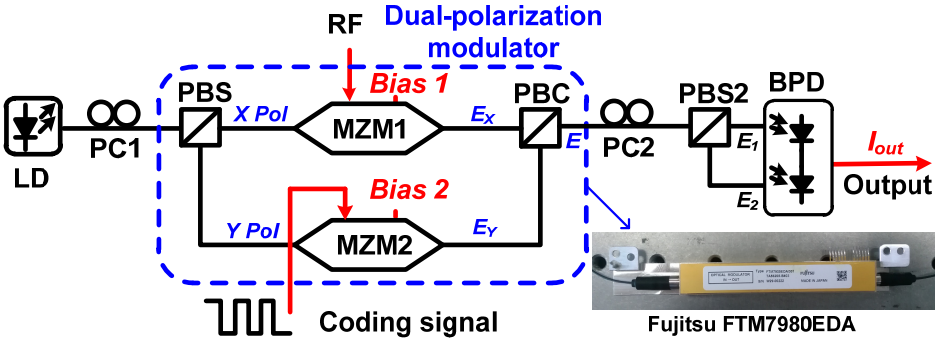


Fig. 1. Schematic diagram of the proposed phase-coded microwave signal generator. LD: laser diode, PC: polarization controller, PBS: polarization beam splitter, PBC: polarization beam combiner, MZM: Mach-Zehnder modulator, BPD: balanced photo-detector.

Figure 1 shows the schematic diagram of the proposed phase-coded microwave signal generator. A laser diode (LD) is applied to generate a continuous wave (CW) light with its polarization adjusted by a polarization controller (PC1). The optical carrier is sent to a dual-polarization modulator which is a commercially available integrated device including two MZMs, a polarization beam splitter (PBS) and a polarization beam combiner (PBC). By adjusting PC1 to let the polarization state of the input light have an angle of 45° to one principal axis of the PBS inside the modulator, the CW light is equally split into two branches in two orthogonal polarizations (i.e., X and Y) after the PBS. The light in each polarization is modulated by MZM1 and MZM2, respectively. Then, the two modulated optical signals are combined by the PBC to generate a polarization multiplexed signal. In the proposed scheme, MZM1 is driven by a single-frequency RF signal and biased at the minimum transmission point to achieve optical carrier-suppressed modulation [18]. After MZM1, the optical field including the ± 1st-order sidebands can be expressed as

$$E_X = A\exp[j2\pi(f_o - f)t] + A\exp[j2\pi(f_o + f)t] \quad (1)$$

#242351 Received 4 Jun 2015; revised 29 Jul 2015; accepted 7 Aug 2015; published 12 Aug 2015

where $A$ is the amplitude of each sideband, $f_o$ is the optical carrier frequency and $f$ is the RF frequency. MZM2 is driven by an electrical non-return-to-zero (NRZ) coding signal to generate an optical binary phase shift keying (BPSK) signal [18], which can be written as

$$E_{\mathrm{Y}} = B\exp\left[j2\pi f_o t + s(t)\right] \tag{2}$$

where $B$ is the amplitude, and $s(t)$ equals either 0 or $\pi$ for bit ' + 1' or '-1' in the coding signal. The output signal from the dual-polarization modulator is $\mathbf{E} = \hat{x}E_{\mathrm{X}} + \hat{y}E_{\mathrm{Y}}$. After the modulator, another PC (PC2) and a PBS (PBS2) is followed. The polarization state of $E_{\mathrm{X}}$ or $E_{\mathrm{Y}}$ is adjusted by tuning PC2 to have an angle of 45° to one principal axis of PBS2. The two output signals from PBS2 are given by

$$E_{1,2} = \sqrt{2}(E_{\mathrm{X}} \pm E_{\mathrm{Y}})/2 \tag{3}$$

Then, the two optical signals are sent to the two input ports of a balanced photodetector (BPD). The generated electrical signals at the two PDs are

$$I_{1,2}(t) = \Re E_{1,2}E_{1,2}^{*} = \frac{\Re}{2}\left\{2A^2 + B^2 + 2A^2\cos(4\pi ft) \pm 4AB\cos[2\pi ft + s(t)]\right\} \tag{4}$$

where $\Re$ is the responsivity of each PD. The output current from the BPD is

$$I_{\mathrm{out}}(t) = I_1(t) - I_2(t) = 4\Re AB\cos[2\pi ft + s(t)] \tag{5}$$

As can be seen in (5), the DC component and the second order harmonics at 2$f$ generated at each PD are removed thanks to the balanced photodetection, and an RF signal centered at $f$ is obtained, of which the phase is modulated by the input coding signal. In this scheme, the frequency and bandwidth of the generated signal can reach tens of GHz, only limited by the bandwidth of the modulator and the BPD. Compared with the previous photonic systems for phase-coded signal generation, the proposed scheme has a very simple structure using only one modulator. Besides, good stability of the generated signal can be ensured because the manipulations of the optical carrier are implemented inside the integrated modulator.

An experiment for the generation of a 2 Gb/s phase-coded signal at 20 GHz is performed to verify the feasibility of the proposed signal generator. A CW light at 1550.51 nm is generated from an LD (TeraXion NLL04) with a power of 15 dBm. The modulator is a dual-polarization BPSK (DP-BPSK) $LiNbO_3$ modulator (Fujitsu FTM7980EDA) which has a 3-dB bandwidth of ~30 GHz and a half-wave voltage of 3.5 V@ 21.5 GHz for each MZM. An RF signal at 20 GHz generated by a microwave signal generator (Agilent E8257D) with a power of 4.5 dBm is applied to drive MZM1, which is biased at the minimum transmission point. After MZM1, an optical carrier-suppressed signal ($E_{\mathrm{X}}$) is generated. Meanwhile, MZM2 is also biased at the minimum transmission point and driven at the full swing to generate an optical BPSK signal ($E_{\mathrm{Y}}$) [18]. The signal driving MZM2 is a 2 Gb/s 13-bit Barker coding signal with a pattern of "+1+1+1+1+1-1-1+1+1-1+1-1+1", which is generated by a pulse pattern generator (PPG). Then, $E_{\mathrm{X}}$ and $E_{\mathrm{Y}}$ are polarization multiplexed at the output of the dual-polarization modulator. After the modulator, an erbium-doped fiber amplifier (EDFA) is applied to boost the optical power, and an optical filter with a 3-dB bandwidth of 67 GHz is followed to remove the amplified spontaneous emission (ASE) noise. After that, the optical signal passes through PC2 and PBS2. By adjusting PC2 to let the polarization states of the two optical signals ($E_{\mathrm{X}}$ and $E_{\mathrm{Y}}$) be aligned to the two principal axes of PBS2, respectively, the two signals can be exported at the two output ports of PBS2. Their spectra are measured by an optical spectrum analyzer (OSA) with a resolution of 0.02 nm. Figure 2(a) shows the spectrum of the generated carrier-suppressed optical signal ($E_{\mathrm{X}}$), where two 1st-order sidebands separated by 40 GHz are generated and the optical carrier is suppressed to be 23 dB lower than the first-order sidebands. Figure 2(b) shows the measured spectrum of the optical BPSK signal ($E_{\mathrm{Y}}$). Due to the un-ideal polarization extinction ratio of PBS2, the two first-

#242351 Received 4 Jun 2015; revised 29 Jul 2015; accepted 7 Aug 2015; published 12 Aug 2015

order sidebands still exist but their power is lower than the optical carrier by more than 30 dB. The eye diagram of the generated optical BPSK signal is measured by an optical sampling oscilloscope, as shown in the inset of Fig. 2 (b), which can confirm that an optical BPSK signal is successfully generated. Finally, the polarization state of $E_X$ or $E_Y$ is adjusted to have an angle of 45° to one principal axis of PBS2. Figure 2(c) shows the optical spectrum measured at one output port of PBS2. The two output signals from PBS2 are directed to the two input ports of a 40 GHz BPD (u2t BPDV2150R-VF-FP), respectively. The waveform of the generated signal is observed by a real-time oscilloscope (Keysight DSO-X 92504A) with a sampling rate of 80 GSa/s.

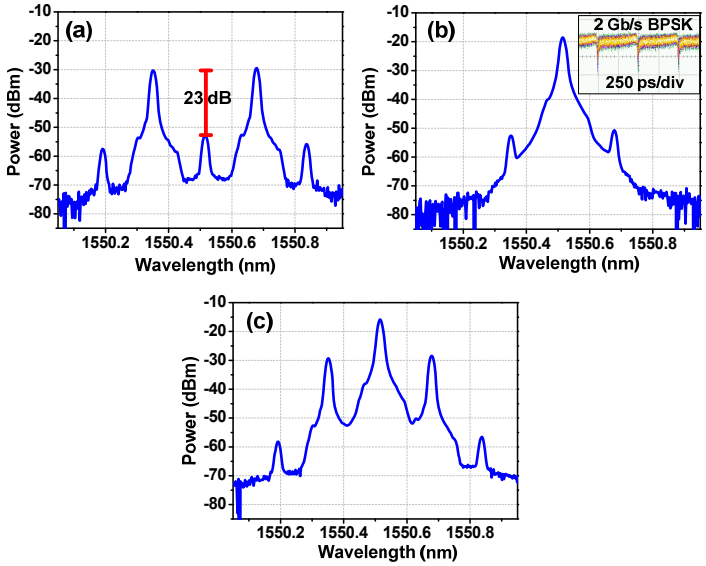


Fig. 2. Measured optical spectra of (a) the carrier-suppressed signal (b) the BPSK signal and (c) the output signal from PBS2. Inset of (b) is the eye diagram of the 2 Gb/s optical BPSK signal.

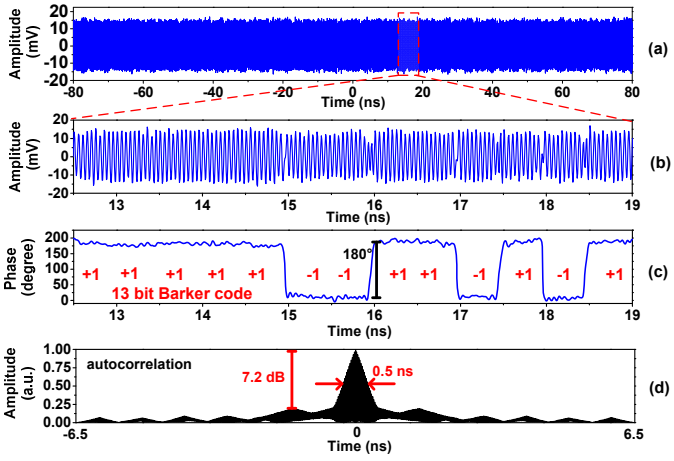


Fig. 3. (a) Measured waveform of the generated 20-GHz phase-coded microwave signal, (b) zoom-in view of the waveform for a duration of 6.5 ns, (c) the recovered phase and (d) the autocorrelation of the 6.5 ns waveform.

#242351 Received 4 Jun 2015; revised 29 Jul 2015; accepted 7 Aug 2015; published 12 Aug 2015

Figure 3(a) shows the measured waveform of the generated 2 Gb/s phase-coded signal at 20 GHz in 160 ns. As can be seen, the signal has equal amplitudes below and above zero without a DC component. The detailed waveform in one period of the 2 Gb/s 13-bit Barker code (6.5 ns) is shown in Fig. 3(b). By applying the phase recovery method based on Hilbert transform [19], the phase of the generated signal can be recovered, as shown in Fig. 3 (c). As can be seen, the recovered phase agrees well with the 13-bit Barker code, and a phase difference of 180° is obviously observed between bit "+1" and bit "-1". Then, the generated signal is sampled every two minutes using the oscilloscope for an hour. Through analysis, the amplitude of the phase-coded signal is found to be nearly constant and the recovered phase is also stable, indicating the good stability of the generated signal. To check the pulse compression ability for radar applications, autocorrelation of the generated 6.5 ns signal is calculated with the result shown in Fig. 3(d). The main-to-sidelobe ratio (MSR) is 7.2 dB and the full width at half maximum of the compressed pulse is 0.5 ns. Thus, a compression ratio of 13 (6.5 ns/0.5 ns) is achieved after pulse compression [1]. By changing the RF frequency, the bit rate and the pattern of the coding signal, the carrier frequency, bandwidth and phase pattern of the generated microwave signal can be tuned independently.

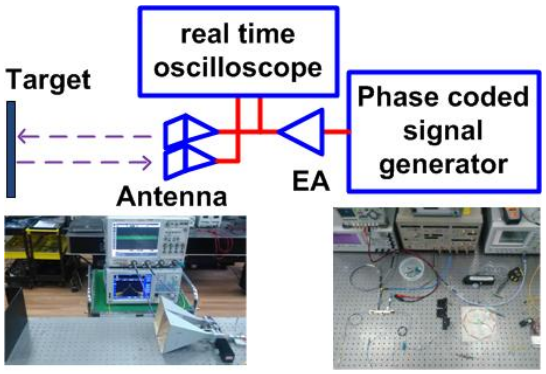


Fig. 4. Schematic diagram of the one-dimension distance measurement system. EA: electrical amplifier.

### 3. One-dimension distance measurement

To further investigate the performance of the proposed signal generator, its application in one-dimension distance measurement is experimentally demonstrated based on the setup in Fig. 4. The generated phase-coded signal is first amplified by an electrical amplifier (SHF 806E) with a gain of 26 dB, and then sent to a horn antenna for air transmission toward a plane metal target. The reflected signal is received by another antenna placed close to the transmitting antenna. The transmitted and received microwave signals are sampled simultaneously by the multi-channel real time oscilloscope. The sampling rate of the oscilloscope is 40 GSa/s. The time delay between the transmitted and received signals can be obtained based on the recorded data, and the distance between the antenna pair and the target can be calculated thereafter. The antennas used in the experiment have a bandwidth of 8-12 GHz, and the transmitted signal is a 1 Gb/s phase coded microwave signal centered at 10 GHz. The coding signal is a 32-bit sequence with a period of 32 ns, which is composed of a 13-bit Barker code followed by another 19-bit sequence with a pattern of "+1-1+1-1+1-1+1-1+1-1+1-1+1-1+1-1+1-1+1-1+1". The 13-bit Barker code is used for distance measurement, and the following 19 bits are used to increase the temporal aperture so as to achieve a large distance measurement range. Here, the pattern of the other 19 bits is chosen to ensure a minimized pattern effect in the generated phase-coded microwave waveform.

Figure 5(a) shows the transmitted and received waveforms measured in 24.5 ns when the actual distance between the antenna pair and the target is 76.4 cm. The 13-bit Barker coded waveform in the received signal is obviously delayed compared with that in the transmitted

#242351 Received 4 Jun 2015; revised 29 Jul 2015; accepted 7 Aug 2015; published 12 Aug 2015

signal. To precisely acquire the time delay, correlations between the 13-bit Barker coded waveform and the transmitted/received signals are calculated. The results are shown in Fig. 6. By calculating the time delay between the two correlation peaks, the time interval corresponding to a round trip transmission between the antenna pair and the target is obtained. Based on this time delay, the distance between the antenna pair and the target can be calculated [1]. In the experiment, multiple distance measurements are performed by changing the target position, and the maximum distance is set as large as the experimental condition permits. The results are: (76.4 cm, 77.5cm), (145.1 cm, 146.4 cm), (175.3 cm, 176.9 cm) and (208 cm, 209.7 cm), where *a* in (*a*, *b*) is the actual distance and *b* is the measured one. The measurement error is found to be 1.1 cm, 1.3 cm, 1.6 cm and 1.7 cm, respectively, which is mainly attributed to the degraded signal-to-noise ratio of the received signal. Besides, the non-ideal compensation of the imbalance between the two channels induced by the cables and other electrical devices also limits the accuracy.

In this experiment, the operation frequency (10 GHz) is constrained by the bandwidth of the antenna. The advantages of photonic systems do not show up since the inexpensive sonar sensors or integrated microwave radars working in the same frequency band already exist and have a good performance. However, the photonic method is expected to find applications in much higher frequency band (e.g., >50 GHz) which is still a challenge for pure electrical technologies.

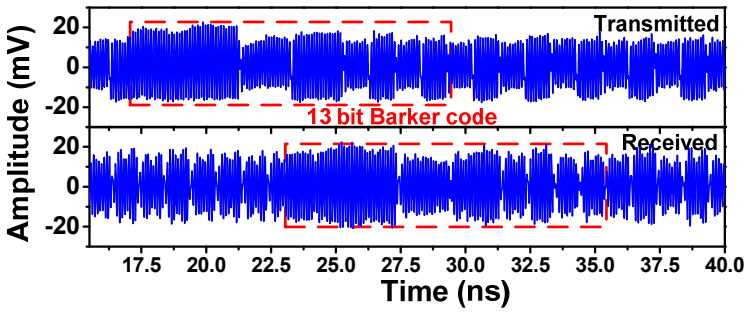


Fig. 5. Measured waveforms of the transmitted (before the amplifier) and received signals in 24.5 ns.

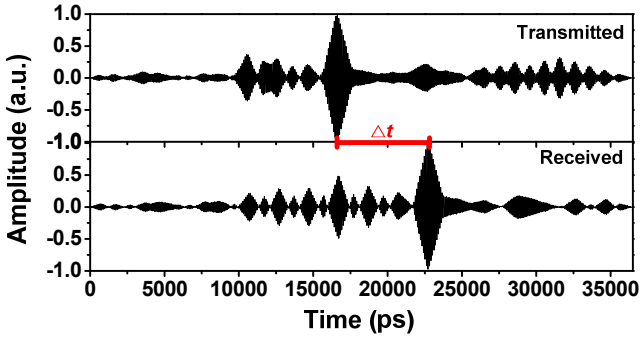


Fig. 6. The correlations between the 13-bit Barker coded waveform and the transmitted/received waveform.

## 4. Conclusions

We have proposed a scheme for photonic generation of phase-coded microwave signals using a dual-polarization modulator, which is simple and reliable compared with the previous photonic schemes. Good performance of the proposed signal generator is verified experimentally through the generation of a 2 Gb/s phase-coded signal at 20 GHz. A one-

#242351 Received 4 Jun 2015; revised 29 Jul 2015; accepted 7 Aug 2015; published 12 Aug 2015

dimension distance measurement experiment is also performed based on the proposed signal generator. An accuracy of no more than 1.7 cm is achieved for the measurement range of ~2 m. The proposed technique is expected to find applications in future radar and communication systems.

**Acknowledgments**

This work was supported in part by the NSFC Program (61401201, 61422108), the 973 Program (2012CB315705), the NSFC Program of Jiangsu Province (BK20140822, BK2012031), the Jiangsu Planned Projects for Postdoctoral Research Funds (1302074B), the Postdoctoral Science Foundation of China (2015T80549, 2014M550290), and the Fundamental Research Funds for Central Universities.

#242351 Received 4 Jun 2015; revised 29 Jul 2015; accepted 7 Aug 2015; published 12 Aug 2015